

# Graphene Supported Platinum Counter Electrode for Dye Sensitized Solar Cells

Ngei Katumo<sup>1</sup>, Simon Waweru Mugo<sup>1</sup>, James Mbiyu Ngaruiya<sup>1</sup>, Paul Kimeu Ngumbi<sup>1,2</sup> and Benjamin Mbaluka John<sup>1,2</sup>

Researcher, Department of Physics, Jomo Kenyatta University of Agriculture and Technology (JKUAT), Nairobi, Kenya<sup>1</sup>

Researcher, Department of Physics and Electronics, South Eastern Kenya University (SEKU), Kitui, Kenya<sup>2</sup>

**ABSTRACT:** A Platinum (Pt) film was prepared on graphene-fluorine-doped tin oxide (FTO) substrate through doctor blade procedure and investigated as a counter electrode (CE) for dye sensitized solar cells (DSSCs). Dye loading of the TiO<sub>2</sub> photoanode was quantitatively evaluated by UV-VIS-NIR spectrophotometry. Upon DSSCs fabrication, the current density-voltage (*I-V*) characteristics were evaluated with simulated solar irradiation of 100 mW/cm<sup>2</sup> (AM 1.5). The DSSC with platinum/graphene (Pt/Gr) as CE exhibited a power conversion efficiency, PCE ( $\eta$ ) of 3.96 % , whereas that of Pt-film CE which had a PCE ( $\eta$ ) of 3.48%. This is a 13.8% improvement in PCE. The Pt/Gr bilayer CE achieved a photocurrent density ( $J_{sc}$ ) of 9.76 mA/cm<sup>2</sup> whereas the Pt-film ( $J_{sc}$ ) had 8.72 mA/cm<sup>2</sup>, which was a 12% improvement. The improvement in performance of Pt/Gr CE is shown to be due to enhanced catalytic activity resulting in reduced charge transfer resistance. Platinum free graphene CE based DSSCs achieved PCE of 1.38%. The fill factor (*FF*) of graphene based DSSC was low at 0.21 and is shown to result from poor catalytic activity leading to high charge transfer resistance at the graphene-electrolyte interface.

**KEYWORDS:** Dye sensitized solar cells, Counter electrode, Graphene, Platinum-Graphene, Catalytic activity, Electron-tunnelling.

## I. BACKGROUND

Dye-sensitized solar cells (DSSCs) are organic cells of respectable energy conversion efficiency, low cost, high durability, easy to fabricate and thus are a promising candidate for solving global environmental and energy problems [1-3]. They were first reported by Regan and Gratzel in 1991 [4, 5]. An increase in their energy conversion efficiency would provide enormous economic advantages. A conventional DSSC comprises of; a working electrode (WE), iodide/triiodide redox system and a counter electrode (CE) [1-3, 6]. The WE consists of the high surface area mesoporous nanocrystalline TiO<sub>2</sub> film which adsorbs the dye molecules. A redox system of iodide/triiodide in organic solvent is sandwiched and sealed between the dye-adsorbed WE and the CE [6]. The solar cells operation principle mimics photosynthesis in that under illumination, the photonic energy strikes the dye which in turn produces excited electron, only and only if the photon has sufficient energy [6]. This involves the dye molecules being photoexcited from their highest occupied molecular orbitals (HOMO) to their lowest unoccupied molecular orbitals (LUMO) state leading to rapid injection of electrons in to the conduction band of the mesoporous nanocrystalline TiO<sub>2</sub> semiconductor. The electrons are then transported to the external circuit [4-6]. Simultaneously, the dye is restored back to its state by the redox system ( $I^- / I_3^-$ ), donating back the electrons thus preventing the recombination of the conduction band electrons with the holes in the dye. Subsequently, the iodide  $I^-$  is regenerated through the reduction of triiodide  $I_3^-$  at the CE by a catalytic material [4-7].

# International Journal of Innovative Research in Science, Engineering and Technology

(An ISO 3297: 2007 Certified Organization)

Vol. 4, Issue 12, December 2015

The CE plays a key role of collecting electrons from the external circuit and electro-catalysing the redox couple regeneration reaction in the DSSC. The CE need be of high catalytic activity to sustain the regeneration of iodide  $I^-$  in order to inhibit electron recombination [4-6]. Conventionally, platinum (Pt) has been the dominant film in CEs for DSSCs because of its outstanding properties such as high conductivity, high catalytic activity towards iodide/triiodide redox reaction and stability [1, 3, 8]. As a means to improve the power conversion efficiency (PCE) of hybrid CEs that incorporate Pt and other composites have been sought. Recently, carbonaceous materials (carbon black, graphene, activated carbon, multi-walled carbon nanotubes), have been demonstrated to have good catalytic activity towards reduction of triiodide, high surface area and high electrical conductivity [9-12] desirable for solar cell CEs. The catalytic activity in these carbonaceous materials is reported to increase with increase in the defect density [9-12].

Graphene has a high optical transmittance of 97.7% in the visible range and high electrical conductivity and has been employed in CEs of DSSCs [6-9, 11, 13]. It is a two-dimensional atomically thin layer of covalently bonded carbon atoms forming hexagonal honey comb lattice [8, 9, 11, 12]. Other unique and desirable properties include; high thermal conductivity ( $\sim 5000 \text{ W m}^{-1} \text{ K}^{-1}$ ), large specific surface area ( $\sim 2630 \text{ m}^2/\text{g}$ ) and its inertness against oxygen and water vapor [1, 6-8]. Embedding Pt on graphene as a CE bilayer increases the PCE. Combining the excellent electronic properties, high surface area and catalytic properties of graphene with the good electronic and catalytic properties of Pt leads to high PCE [2, 8-10, 14]. The Pt/Gr composite improves electron kinetics and collection by the triiodide through creating an electronegative surface potential.

The various techniques of producing graphene have been reported to produce different results in conversion efficiency when used as CEs [2, 6-8, 13, 15]. In this study, CVD graphene on FTO is used to fabricate standalone DSSCs. Pt/Gr CEs are fabricated and shown to enhance the efficiency of DSSCs by 13.8%. The graphene films were analysed from an optical and structural point of view using Raman Spectroscopy and the UV-VIS- NIR Spectrophotometry.

## II. EXPERIMENTAL PROCEDURE

### Preparation of Counter Electrodes

Prior to use, the FTO  $\text{SnO}_2:\text{F}$  glass substrates (2.0 cm x 1.5 cm, sheet resistance,  $7 \Omega/\text{sq}$ , Xinyan Technology Co. Limited, China) were cleaned using acetone (purity 99.5%), ethanol (purity 99.5%) and deionized water sequentially for 5 minutes in each step. The CVD graphene (coverage  $>98\%$ ) on the FTO  $\text{SnO}_2:\text{F}$  glass substrates (Graphene Laboratories, USA) were soaked in ethanol for 5 minutes, rinsed with deionized water for 5 minutes and then dried with pressurized air. For Pt based CEs, the cleaned FTO  $\text{SnO}_2:\text{F}$  glass substrates were coated on the conductive side with a wet layer of Pt precursor paste (Platisol T/SP pore size, 15-20 nm, Solaronix, Switzerland) through the doctor-blade procedure. The Pt/Gr counter electrode films were prepared through doctor-blading the cleaned graphene film with the Pt precursor paste. The Pt and Pt/Gr films were then kept for 20 minutes in a clean box to enhance homogeneity after which they were heat treated at a temperature ramp of  $5^\circ\text{C}/\text{min}$  up to  $150^\circ\text{C}$  and then sintered at  $400^\circ\text{C}$  for 30 minutes to activate the Pt film.

### Preparation of Working Electrodes

Nanocrystalline  $\text{TiO}_2$  films were prepared by slot-coating titanium nanoxide T/SP (18% wt, 15-20 nm, Solaronix, Switzerland) on the cleaned FTO  $\text{SnO}_2:\text{F}$  glass substrates. The drying process began with twenty minute ambient temperature, to enhance homogeneity of the film, followed by a temperature ramp,  $5^\circ\text{C}/\text{min}$  up to  $175^\circ\text{C}$  in a furnace. The photoanodes were then sintered at  $450^\circ\text{C}$  for 30 minutes and let to cool in the furnace. They were then dye-sensitized through immersing them in 0.5 mM cis-diisothiocyanato-bis (2,2'-bipyridyl-4,4'-dicarboxylato) ruthenium(II) bis (tetrabutylammonium), the so called N719 dye for 24 hours to maximize dye loading. Dye loading was quantitatively evaluated by UV-VIS-NIR spectrophotometry.

# International Journal of Innovative Research in Science, Engineering and Technology

(An ISO 3297: 2007 Certified Organization)

Vol. 4, Issue 12, December 2015

## Fabrication of DSSCs and Characterization

The dye-covered TiO<sub>2</sub> electrode and the different CEs were assembled in to a sandwich type of cell using a Dupont surlyn (Meltonix 1170-25 Solaronix, Switzerland) sealant with a micro-space at 80 °C. The redox couple, iodine/triiodide, 30 mM of ionic liquid, lithium salt, pyridine derivative, thiocyanate on acetonitrile solvent, (Iodolyte HI-30, Solaronix, Switzerland), was via injected through the micro-space after which it was sealed using the sealant melt. The cells were kept in the dark for 24 hrs. The DSSCs were then characterized by analysing the I-V characteristics obtained through applying an external bias on the DSSCs in a dark room. A 450 W halogen lamp adjusted to an intensity output of 100 mW/cm<sup>2</sup> at the DSSCs' surface was used as the light source. A solar power meter TM206 (3T0-3-1, Tenmars Taiwan) and a single crystal Si photodiode was used to maintain the irradiation on the DSSCs at 1 sun, 100 mW/cm<sup>2</sup>. Prior to taking measurements, the cells were covered with a black mask fitted around the active area of 0.64 cm<sup>2</sup>. The I-V characteristics were obtained through applying an external bias on the DSSCs in a dark room to avoid stray light. The photovoltaic (PV) parameters, open-circuit voltage (*V<sub>oc</sub>*) short-circuit current density, *J<sub>sc</sub>*, and the fill factor (*FF*) were extracted from the *I-V* curve and used to calculate the DSSC's power conversion efficiency,  $\eta$ .

$$\eta = \frac{P_{max}}{P_{in}} \times 100\% = \frac{FF \times V_{oc} \times J_{sc}}{P_{in}} \times 100\% \dots\dots\dots 1$$

Where *p<sub>in</sub>* is the input power as measured by the solar meter and cross referenced with a Si photodiode while the *FF* is given by;

$$FF = \frac{J_m V_m}{J_{sc} V_{oc}} \dots\dots\dots 2$$

### III. RESULTS AND DISCUSSION

The absorption spectrum of dye loading is as shown in Fig. 1(a). The N719 dye loading substantially increases the absorption in the wavelength range; (400-600 nm). The highest absorption occurs in 540 nm. The loading is lowest in the infra-red region a phenomena of the FTO and the N719 dye which have reduced absorption potential of the Infra-red. The thicknesses of the WE were 8.5-9.5 μm. This thickness is within the desired thickness for TIO<sub>2</sub> DSSC to function optimally [16].

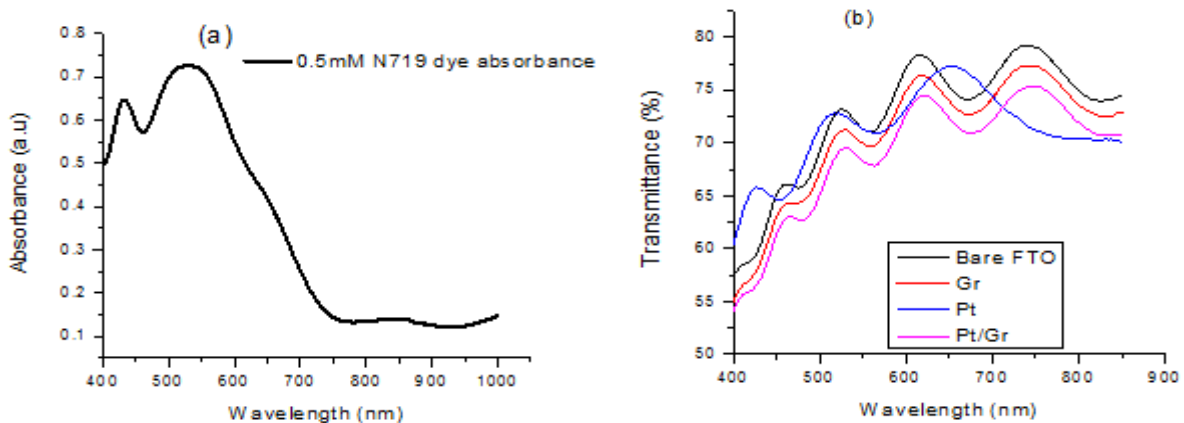


**Figure 1:** UV-Vis NIR Spectrum: (a) the absorption spectrum of 0.5 mM N719 dye in the visible and Infrared region in arbitrary units. (b) The transmission spectra of the bare FTO, Gr on FTO and Pt/Gr counter electrodes. The FTO, Gr and Pt/Gr transmittances indicate a uniform decrease in transmittance trend.

## International Journal of Innovative Research in Science, Engineering and Technology

(An ISO 3297: 2007 Certified Organization)

Vol. 4, Issue 12, December 2015

The optical transmittance of bare FTO, graphene, Pt and Pt/Gr CEs is as shown in Fig. 1 (b). Graphene optical transmittance in this case displays the expected optical density of  $\sim 2.3\%$  from the bare FTO. All the CEs show a transmittance above 55% with a low variation in the transmittance of graphene and Pt/Gr CEs. The high and constant optical transmittances of above 70% in the most of the visible range indicate that Pt/Gr can be used for rear illumination and in window applications. The results indicate that graphene does not cause optical interference on FTO. Similarly Pt on graphene does not cause any optical interference as the transmission spectra exhibits a similar trend depicting the slight reduction in transmission as expected. However, the Pt on FTO causes optical interference hence the trend is dissimilar to the bare FTO one. The optical densities indicate that the cells can be used for back illumination and hence can be used in window based DSSCs.

The photocurrent density-voltage curve of, graphene CE, Pt/Gr and reference Pt DSSCs are shown in Fig. 2. The  $V_{oc}$ ,  $J_{sc}$ ,  $FF$  and  $\eta$  values (Table 1) indicate that the  $FF$  is independent of the  $V_{oc}$ ,  $J_{sc}$ , for DSSCs. Further, there is no correlation between the  $V_{oc}$ ,  $J_{sc}$  and  $FF$  in all the DSSCs. However, the  $FF$  is observed as core to the overall conversion efficiency of the cells unlike the  $V_{oc}$  and  $J_{sc}$ .

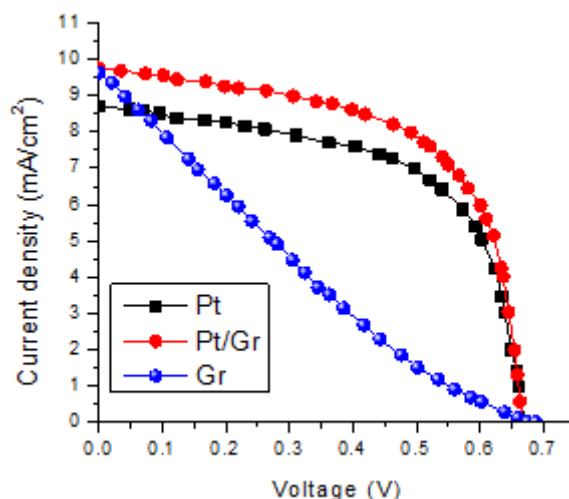


**Figure 2:**  $I$ - $V$  characteristics of DSSCs with different CEs measured at  $100 \text{ mW/cm}^2$ , (AM 1.5) illumination

The graphene based CE exhibits a PV performance with  $V_{oc}$ ,  $J_{sc}$ ,  $FF$  and  $\eta$  being 0.675 V, 9.63 mA /cm<sup>2</sup>, 0.21 and 1.38% respectively. For the Pt reference cell, the PV parameters are 0.670 V, 8.72 mA /cm<sup>2</sup>, 0.60 and 3.48% for  $V_{oc}$ ,  $J_{sc}$ ,  $FF$  and PCE respectively. These results agree with what has been previously reported [2, 6, 7]. Compared to Pt DSSC, the  $V_{oc}$  and  $J_{sc}$  values of the graphene DSSC are high. However, the  $FF$  is only 35% that of the reference Pt DSSC. The graphene DSSC achieves a PCE of 1.38 % which is a 62.1% decrease in respect to the Pt DSSCs. This low  $FF$  is as a result of poor catalytic activity in the junction of graphene CE and the electrolyte arising from large charge transfer resistance ( $R_{CT}$ ) [13, 20, 30].

Poor diffusion of the  $I^- / I_3^-$  redox species in the pores of graphene contributes to the high  $R_{CT}$  in the graphene - electrolyte interface hence the low  $FF$  [21, 22]. The large  $R_{CT}$  leads to longer redox reaction times in the graphene CE hence amplification of charge recombination between electrons excited from the dye to the conduction band of TiO<sub>2</sub> and the  $I_3^-$  ions [13]. The low  $FF$  causes a potential drop across the Gr/FTO interface due to sluggish electron transfer leading to a low PCE [30]. It is however interesting to note that the  $V_{oc}$  and the  $J_{sc}$  is higher than in Pt. The  $V_{oc}$  of DSSCs is dictated by the quasi-Fermi level of the TiO<sub>2</sub> and the potential of the redox couple [31]. On the contrary, the  $J_{sc}$  arises from the electron injection efficiency from the dye to the conduction band of TiO<sub>2</sub> and the efficiency of charge collection [31]. These results coincide with what has previously been reported [21, 22].

## International Journal of Innovative Research in Science, Engineering and Technology

(An ISO 3297: 2007 Certified Organization)

Vol. 4, Issue 12, December 2015

**Table 1:** PV performance of Pt, Pt/Gr and graphene CE based DSSCs showing the  $V_{oc}$ ,  $J_{sc}$ ,  $FF$  and PCE ( $\eta$ )

CE	$V_{oc}$ (V)	$J_{sc}$ mA/cm <sup>2</sup>	$FF$	$\eta$ %
Pt	0.670	8.72	0.60	3.48
Pt/Gr	0.670	9.76	0.61	3.96
Gr	0.675	9.63	0.21	1.38

The Pt/Gr composite CE based DSSC shows a 12% improvement in  $J_{sc}$  and 13.8% improvement in PCE with respect to the Pt-film based DSSC. Its PV parameters are 0.670 V, 9.76 mA/cm<sup>2</sup>, 0.61 and 3.96% for  $V_{oc}$ ,  $J_{sc}$ ,  $FF$  and  $\eta$  respectively. The observable difference in the PV parameters of the Pt/Gr CE based DSSC with respect to Pt cell is only in the  $J_{sc}$ . The Pt/Gr and Pt CE based DSSCs have similar  $V_{oc}$  and  $FF$  but different  $J_{sc}$  which thus is the contributing factor to the 13.8% improvement in PCE. The Pt/Gr based CE therefore has insignificant influence on the  $V_{oc}$  and  $FF$  of the DSSCs. Unlike the Gr based DSSC, which has a low  $FF$ , the Pt/Gr CE based DSSC has high  $FF$  indicating comparable catalytic activity towards the reduction of the redox species. This enhancement is as a result of induced negative interfacial surface potential on the platinum surface which was ~50 nm.

In theory, when Pt is contacted to graphene, Pt develops a negative surface charge which is favourable for its catalytic activity in the reduction of the electronegative triiodide. This is due to the work function (WF) difference between the two materials with graphene having ~4.6 eV and platinum having ~5.7 eV [18, 25]. As a result, when a Pt/Gr interface is formed, electrons migrate from the low WF metal (graphene) to the high WF metal (Pt), as illustrated in Fig. 3. This leads to electron tunneling due to the surface dipole which supplements the normal electrochemical process in the electrode-electrolyte interface. The  $E_F$  is the fermi level,  $E_{vac}$  is the vacuum energy level, CB is the conduction band and coincides with  $E_F$  for metals. The 1.5 eV WF difference causes surface charges which enhance triiodide reduction as shown on the platinum surface.

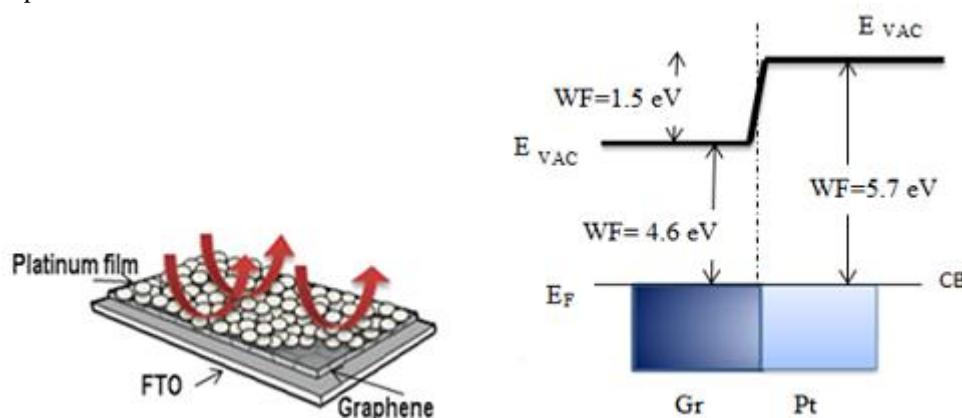


**Figure 3:** The workfunction model of Platinum-Graphene interface.

The charge transfer creates a negative surface potential on the Pt surface which favours backward electron transfer kinetics. This would lead to the electronegative redox couple triiodide species picking electrons easier as compared to the case of absence of a negative surface potential. The picked electrons on the Pt surface are easily replaced by the superconducting graphene. This phenomenon leads to enhanced catalytic activity of platinum on graphene and reduced recombination due to high concentrations of  $I_3^-$  [19]. The electronegative Pt surface of Pt/Gr CE has been reported to have low contact resistance compared to the bare Pt based CE [13, 21-24, 28]. Further, graphenes' high electrical conductivity and high specific area property as opposed to FTO surface has been reported to enhance Pt catalytic activity [9, 21-24, 28]. It has been reported that, the platinum film on graphene is sufficiently dispersed and stabilized



for maximum accessibility of the electrolyte [17, 23, 26, 27]. Further, the diffusion of the redox species in the pores of platinum is maximized by the increased surface area of Pt resting on graphene [21, 23, 29].

Based on Fig 3 model, the WF changes in the CE would favour electron collection after dye excitation. The electron and current path after the dye absorbs a photon and releases an electron is as illustrated in Fig. 4. The high value of Pt WF is core in ensuring the surface has sufficient electrons for fast reduction of the redox species. Thus, the high  $J_{sc}$  in Pt/Gr is ascribed to the introduced surface charge potential that leads to enhanced catalytic activity. The Pt/Gr also provided larger diffusion coefficient leading to a facile electron transfer hence the high  $J_{sc}$  [28].

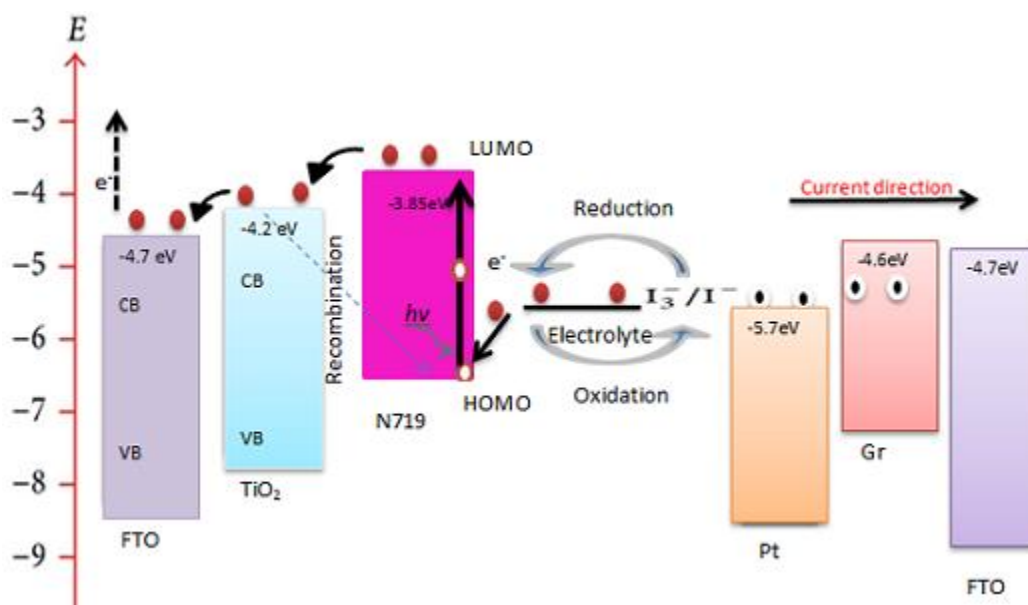


**Figure 4:** The electron process of DSSC with various energy levels of its components: the conduction and valence band of FTO and TiO<sub>2</sub>, the HOMO and LUMO levels of N719 Dye, the redox couple and the current direction.

The overall effect of the Pt/Gr bilayer CE is thus to introduce a negative surface charge on Pt, increase the surface area and enhance electron transfer to the redox species. These findings are consistent with what has been previously reported [9, 21, 22, 28].

#### IV. CONCLUSION

A Pt/Gr CE was developed and shown to improve the photocurrent and the PCE by 12% and 13.8% respectively. The Pt/Gr CE based DSSC exhibited a PCE of 3.96%. This 13.8% improvement has been shown to be due to the negative surface potential, which enhances the catalytic activity of Pt, the electron tunnelling aspect due to WF difference, the lower charge transfer resistance on the Pt/Gr CE-electrolyte interface and the increased surface area for the platinum film. The electronegative redox species easily picked electrons on the Pt surface hence inhibiting chances of electron recombination in the DSSC. Further, graphene based CE exhibited PCE of 1.38% which is lower than that of the Pt standalone electrode by 60.34%. This performance is consistent with what has previously been reported.

# International Journal of Innovative Research in Science, Engineering and Technology

(An ISO 3297: 2007 Certified Organization)

Vol. 4, Issue 12, December 2015

## REFERENCES

- [1]. Chen L., Hsu C., Chan P., Zhang X. and Huang C., "Improving the performance of dye-sensitized solar cells with TiO<sub>2</sub>/graphene/ TiO<sub>2</sub> sandwich structure", *Nanoscale Research Letters*, Vol. 9, pp. 380, 2014.
- [2]. Ping-Jian P., Kai C., Yuan-Fu C., Ze-Gao W., Xin H., Jing-Bo L., Jia-RUi H. and Wang-Li Z., "Low platinum loading ptNPs/graphene composite catalyst with high electrocatalytic activity for dye sensitized solar cells", *Chinese physics B*, Vol. 11, no. 21, pp. 118101, 2012.
- [3]. Wu J., Li Y., Tang Q., Yue G., Lin J., Huang M., and Meng L., "Bifacial dye-sensitized solar cells: A strategy to enhance efficiency on transparent polyaniline electrode", *Scientific reports*, Vol. 4, No. 4023, 2014.
- [4]. Gratzel M., "Molecular photovoltaics that mimic photosynthesis", *Pure Applied Chemistry*, Vol. 73, No. 3, pp. 459-467, 2001.
- [5]. Sedghi A., Miankushki H.N., "Effect of multi walled carbon nanotubes as counter electrode on dye sensitized solar cells", *International Journal of Electrochemical Science*, Vol. 9, pp. 2029-2037, 2014.
- [6]. Dodoo-Arhin D., Fabiance M., Bello A. and Manyala N., "Graphene: Synthesis, transfer, and characterization for dye sensitized solar cells applications", *Industrial and Engineering Chemistry Research*, Vol. 52, pp. 14160-14168, 2013.
- [7]. Kaniyoor A. and Ramaprabhu S., "Thermally exfoliated graphene based counter electrode for low cost dye sensitized solar cells", *Journal of Applied Physics*, Vol. 109, pp. 124308, 2011.
- [8]. Ye M., Wen X., Wang M., Iocozzia J., Zhang N., Lin C. and Lin Z., "Recent advances in dye-sensitized solar cells: from photoanodes, sensitizers and electrolytes to counter electrodes", *Materials today*, Vol. 00, No. 00, 2014.
- [9]. Cruz R., Tanaka D. A. P. and Mendes A., "Reduced graphene oxide films as transparent counter-electrodes for dye sensitized solar cells", *Solar Energy*, Vol. 86, pp. 716-724, 2012.
- [10]. Al-bahrani M.R., Ahmad W., Mehne H.F., Chen Y., Cheng Z. and Gao Y., "Enhanced electrocatalytic activity by RGO/MWCNTS/NiO counter electrode for dye-sensitized solar cells", *Nano-Micro letters*, Vol. 7, No. 3, pp. 298-306, 2015.
- [11]. Wang H. and Hu Y.H., "Graphene as a counter electrode material for dye-sensitized solar cells", *Energy and Environmental Science*, Vol. 5, pp. 8182-8188, 2012.
- [12]. Zhang D.W., Li X.D., Li H.B., Chen S., Sun Z., Yin X.J. and Huang S.M., "Graphene-based counter electrode for dye-sensitized solar cells", *Carbon*, Vol. 49, No. 15, pp. 5382-5388, 2011.
- [13]. Cheng C., Lin C., Shan C., Tsai S., Lin K., Chang C. and Chien S., "Platinum-graphene counter electrodes for dye sensitized solar cells", *Journal of Applied Physics*, Vol. 114, pp. 014503, 2013.
- [14]. Ellis C.T., Stier A. V., Kim M. Tischler J. G., Glaser E. R., Myers-Ward R. L. Tedesco J.L., Eddy C.R., Gaskill D.K. and Cerne J., "Magneto-optical fingerprints of distinct graphene multilayers using the giant infrared Kerr effect", *Scientific Reports*, Vol. 3, pp. 3143, 2013.
- [15]. Li X., Zhu Y., Cai W., Borysiak M., Han B., Piner R., Colombo L. and Ruoff R.S., "Transfer of large-area graphene films for high-performance transparent conductive electrodes", *Nano letters*, Vol. 9, No. 12, pp. 4359-4361, 2009.
- [16]. Baglio V., Girolamo M., Antonucci V., Arico A. S., "Influence of TiO<sub>2</sub> thickness on the electrochemical behaviour of dye-sensitized solar cells", *International Journal of Electrochemical Science*, Vol. 6, pp. 3375-3384, 2011.
- [17]. Tan C., Huang X. and Zhang H., "Synthesis and applications of graphene-based noble metal nanostructures", *Materials Today*, Vol. 16, pp. 29-36, 2013.
- [18]. Seo J.K., Bong J., Cha J., Lim T., Son J., Park S.H., Hwang J., Hong S. and Ju S., "Manipulation of graphene work function using a self-assembled monolayer", *Journal of Applied Physics*, Vol. 116, pp. 084312, 2014.
- [19]. Boschloo G. and Hagfeldt A., "Characteristics of the iodide/triiodide redox Mediator in Dye Sensitized Solar Cells", *Accounts of Chemical Research*, Vol. 42, pp. 1819-1826, 2009.
- [20]. Jeng M., Wang Y., Chang L. and Chow L., "Particle size effects of TiO<sub>2</sub> layers on the solar efficiency of dye-sensitized solar cells", *International Journal of Photoenergy*, Vol. 2013, pp. 563897, 2013.
- [21]. Gong F., Wang H. and Wang Z., "Self-assembled monolayer of graphene /Pt as a counter electrode for efficient dye-sensitized solar cell", *Physical Chemistry Chemical Physics*, Vol. 13, pp. 17676-17682, 2011.
- [22]. Yen M., Teng C., Hsiao M., Kiu P., Chuang W., Ma C., Hsieh C., Tsai M. and Tsai C., "Platinum nanoparticles/graphene composite catalyst as a novel composite counter electrode for high performance dye-sensitized solar cells", *Journal of materials chemistry*, Vol. 21, pp. 12880-12888, 2011.
- [23]. Blanita G. and Lazar M. D., "Review of graphene-supported metal nanoparticles as new and efficient heterogeneous catalyst". *Micro and Nanosystems*, Vol. 5, No. 2, pp. 138-149, 2013.
- [24]. Sur U.K. "Graphene: A rising star on the horizon of material science", *International Journal of electrochemistry*, Vol. 2012, pp. 237689, 2012.
- [25]. Gossenberger F., Roman T., Forster-Tornigol K., Grob A., and Behm R.J., "Change of the work function of Platinum electrodes induced by halide adsorption", *Beilstein Journal of Nanotechnology*, Vol. 5, pp. 152-161 2014.
- [26]. Neto, A. H. C., Guinea, F., Peres, N., Novoselov, K. & Geim, A., "The electronic properties of graphene", *Reviews of Modern Physics*, Vol. 81, pp. 109-162, 2009.
- [27]. Garg R., Dutta N.K. and Choudhury R., "Work Function Engineering of Graphene", *Nanomaterials*, Vol. 4 pp. 267-300, 2014.
- [28]. Yue G., Wu J., Xiao Y., Huang M., lin J., Fan L. and lan Z., "Platinum/graphene hybrid film as a counter electrode for dye-sensitized solar cells", *Electrochimica Acta*, Vol. 92, pp. 64-71, 2013.
- [29]. Seger B., Kamat P. V., "Electrocatalytic active graphene-platinum nanocomposites. Role of 2-D carbon support in PEM fuel cells", *The Journal of Physical Chemistry C*, Vol. 113, pp. 7990-7995, 2009.
- [30]. Yang W., Xu X., Tu Z., Li Z., You B., Li Y., Raj S.I., Ynag F., Zhang L., Chen S., Wang A., "Nitrogen plasma modified CVD grown graphene as a counter electrodes for bifacial dye-sensitized solar cells", *Electrochimica Acta*, Vol. 173, pp. 715-720, 2015.



ISSN(Online): 2319-8753  
ISSN (Print): 2347-6710

## **International Journal of Innovative Research in Science, Engineering and Technology**

*(An ISO 3297: 2007 Certified Organization)*

**Vol. 4, Issue 12, December 2015**

- [31]. Allegrucci A., Lewcenko A.N., Mozer A.J., Dennany L., Wagner p., Officer D.L., Sunahara K., Mori S. and Spiccia L., "Improved performance of porphyrin-based dye sensitized solar cells by phosphinic acid surface treatment", Energy and Environmental Science. Vol. 2. pp. 1069-1073, 2009.